Journal of the Physical Society of Japan **94**, 053702 (2025) **Letters**
https://doi.org/10.7566/JPSJ.94.053702

Control of the Electronic States of the Organic Conductor α-(BEDT-TTF)$_2$I$_3$ by Uniaxial Tensile and Compressive Strain

Takako Konoike*, Shinya Uji, Yuya Hattori, and Taichi Terashima

Research Center for Materials Nanoarchitectonics (MANA), National Institute for Materials Science (NIMS), Tsukuba, Ibaraki 305-0003, Japan

(Received March 11, 2025; accepted April 9, 2025; published online April 25, 2025)

We developed a sample mounting method that enables the use of a piezoelectric-based strain cell, allowing us to measure the electrical resistance of the organic conductor α-(BEDT-TTF)$_2$I$_3$ under uniaxial tensile and compressive strain. The metal–insulator (M–I) transition temperature changes with the application of uniaxial strain, exhibiting large anisotropy with respect to the strain direction. We successfully controlled the electronic states from the metallic to the insulating state by the continuous application of uniaxial strain at low temperatures. The strain dependence of the resistance and elastoresistance exhibits characteristic behavior around the M–I transition temperature. Based on previous X-ray diffraction measurements, we consider that the libration of BEDT-TTF molecules plays a crucial role in the characteristic behavior around the phase transition.

Pressure has long been employed as an effective tool for investigating the physical properties of strongly correlated electron systems. Most of these studies have been conducted under hydrostatic conditions, where isotropic pressure is applied to the sample. For experiments up to about 3 GPa, clamp-type pressure cells using liquids such as oil as pressure-transmitting medium are commonly used. However, when varying the applied pressure using this method, the pressure cell must be removed from the cryostat, making it impossible to vary the pressure continuously. Therefore, it is difficult to precisely investigate the pressure dependence of phase transitions. In addition, experiments under hydrostatic pressure cannot determine which direction of pressure is most effective in altering electronic properties. Recently, Hicks et al. developed a uniaxial strain device using a piezoelectric actuator.[1] This apparatus enables continuous strain control at low temperatures and can apply both uniaxial compression and tension. Using this device, the symmetry of the unconventional superconducting gap[2] and the electronic nematic state, where the rotational symmetry of the system is broken, have been intensively studied.[3–5] This apparatus has been used for inorganic materials after processing them into long, thin plates. On the other hand, applying this technique to organic materials is challenging because single crystals are fragile and small.

As a method for applying uniaxial pressure to organic conductors, the epoxy-crystal method, which combines a clamp-type cell with a sample embedded in cylindrical epoxy resin, has been developed.[6] However, as mentioned above, continuous pressure adjustment is not possible with a clamp-type cell. Another reported method applies effective uniaxial strain continuously by bending a flexible substrate with an organic conductor on it,[7,8] but it requires transferring an ultrathin sample (a few hundred nanometers thick) onto a microfabricated electrode. In this study, we developed a sample mounting method that enables the use of a piezoelectric-based strain cells for single crystals of organic conductors as well as inorganic materials. Using this device, we investigated α-(BEDT-TTF)$_2$I$_3$ and successfully controlled its electronic state. This compound is known to form a Dirac electron system when the metal–insulator (M–I) transition is suppressed under high hydrostatic pressure above 12 kbar.[9,10] We discuss the relationship between the M–I transition and the libration of BEDT-TTF molecules based on resistance behavior near the phase transition temperature.

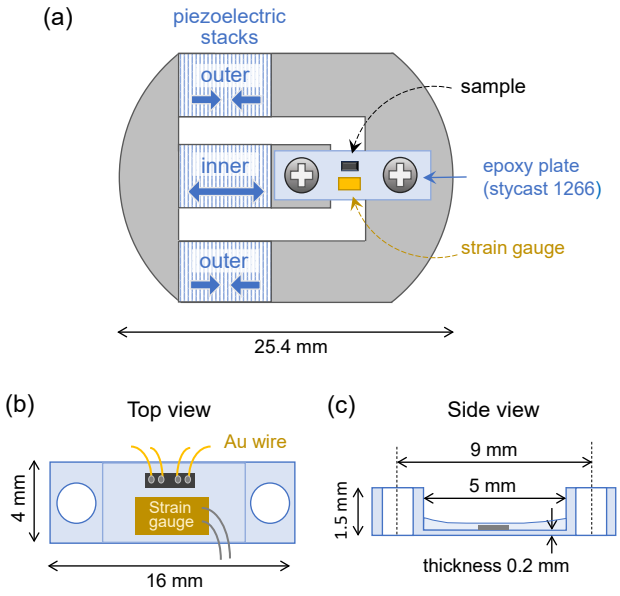

Fig. 1. (Color online) (a) Schematic illustration of a piezoelectric-based strain cell. The arrows on the outer and inner piezoelectric stacks indicate the direction of stack movement when compressive strain is applied to the sample. (b, c) Top view and side view of the epoxy plate, respectively.

Uniaxial strain experiments were performed using a piezoelectric-based strain cell [Razorbill Instruments FC100, Fig. 1(a)]. Single crystals of α-(BEDT-TTF)$_2$I$_3$ were grown by electrochemical oxidation.[11] We selected thin crystals with a typical size of $0.8 \times 0.3 \times 0.02$ mm^3. Gold wires (10 µm in diameter) were attached to the sample with carbon paste for electrical resistance measurements. First, a plate of epoxy resin (Stycast 1266), which has elasticity similar to that of organic conductors, was prepared. To enable the application of stronger strain, the plate was thinned to a thickness of 0.2 mm, leaving only the screw-fastening areas for the device. The sample and the strain gauge with electrodes were placed on the plate [Fig. 1(b)] and embedded in the epoxy resin by coating them with epoxy, as shown in

Fig. 1(c). To prevent damage to the sample from the uncured epoxy, the surface of the sample was pre-coated with enamel. Finally, the epoxy plate was mounted on the strain cell with screws, as shown in Fig. 1(a). Uniaxial compressive strain was generated by applying positive and negative voltages to the outer and inner piezoelectric stacks, respectively, while uniaxial tensile strain was generated by applying the opposite voltages. In this apparatus, the three stacks are arranged so that the thermal contraction effect of the piezoelectric elements is canceled out. Electrical resistivity was measured using a standard four-terminal method, and the strain was monitored by a strain gauge placed next to the sample. The strain cell was attached to the bottom of the probe and inserted into the ^{4}He cryostat. Uniaxial compression and tension could be applied repeatedly as long as the sample remained properly fixed to the epoxy substrate.

In α-(BEDT-TTF)$_2$I$_3$, the M–I transition occurs at 135 K under ambient pressure,[12] and it has been shown that the insulating ground state is charge ordered (CO) state induced by the nearest neighbor Coulomb interaction.[13–16] In this compound, an anisotropic triangular lattice is formed, as shown by the dotted lines in Fig. 2(a). At room temperature, the unit cell (thin lines) contains three crystallographically independent molecules: A, B, and C. Molecule A′ is equivalent to A owing to the inversion symmetry. In CO state below $T_{CO} = 135$ K, molecules A and A′ become inequivalent, and a horizontal type CO state stabilizes, where molecules A and B are charge rich, while molecules A′ and C are charge poor [Fig. 2(b)].

Figures 2(c) and 2(d) show the temperature dependence of the resistance of α-(BEDT-TTF)$_2$I$_3$ under uniaxial strain along the a- and the b-axes, with a constant voltage applied to the piezoelectric stacks, respectively. Here, the strain generated by the applied voltage varies slightly with temperature; the strain applied to the sample decreases by approximately 10% for every 10 K drop in temperature. Therefore, each curve in Figs. 2(c) and 2(d) does not strictly correspond to the result under the same strain intensity. The intensity of strain in each curve was determined at 130 K. Under the a-axis strain, the transition temperature T_{CO} is suppressed by compressive strain, while it increases with tensile strain, as shown in Fig. 2(c). The results indicate that approximately 0.3% tensile or compressive strain can increase or decrease T_{CO} by about 10 K, respectively. This behavior resembles the results observed under hydrostatic pressure,[17,18] suggesting that this compound is highly sensitive to pressure along the a-axis. The effect of 0.3% compression along the a-axis is nearly equivalent to that of 1.4 kbar of hydrostatic pressure. Using the epoxy-crystal method,[6] a decrease in resistance suggesting superconductivity has been observed at 7.2 K under a-axis uniaxial pressure of 2 kbar.[19] Additionally, a transition to a Dirac electron state has been observed under an effective a-axis strain induced by bending the substrate.[8] In our measurements down to 1.5 K, neither phenomenon was observed, suggesting that a larger compressive strain is required to realize these states. On the other hand, the strain dependence of T_{CO} qualitatively agrees with the results obtained by both experimental methods. The stabilization of the CO state observed under the a-axis tensile strain cannot be achieved by using a clamp-type cell, which can only apply

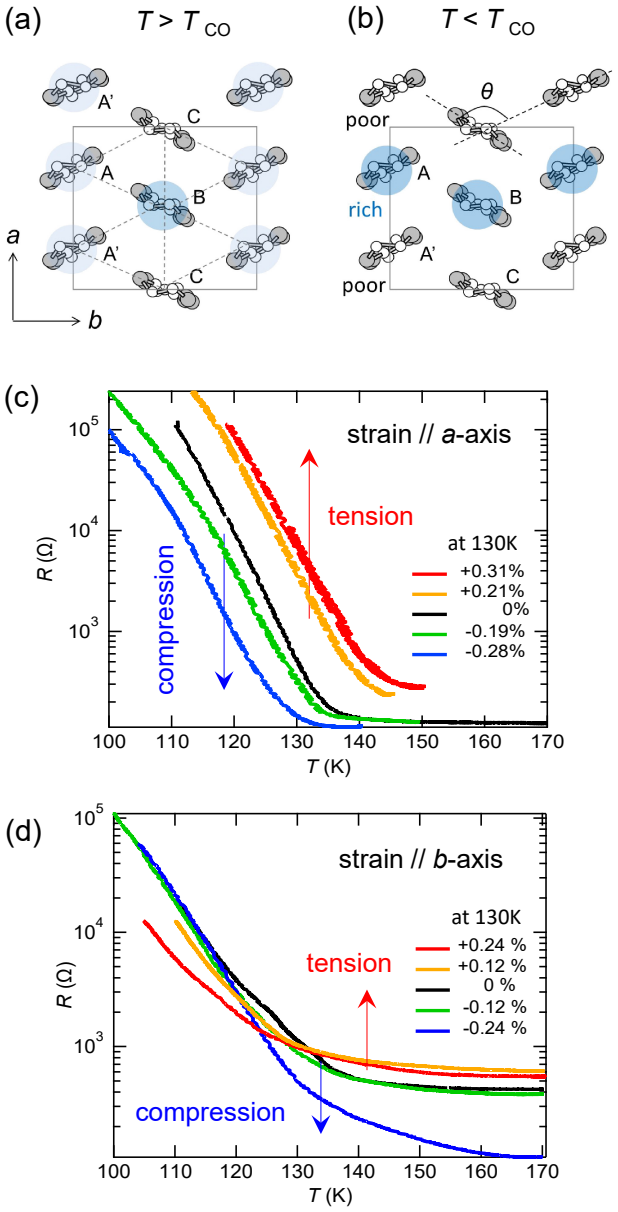

Fig. 2. (Color online) (a, b) Arrangement of BEDT-TTF molecules in the conducting layer of α-(BEDT-TTF)$_2$I$_3$ above and below T_{CO}, respectively. Above T_{CO}, molecules A and A′ in the unit cell (thin lines) are crystallographically equivalent due to inversion symmetry. (c, d) Temperature dependence of resistance under the a- and the b-axes strain, respectively. The strain intensity in each curve was determined at 130 K.

compressive stress. This highlights the importance of using this device to elucidate the electronic properties of the material, and it is even expected that a new electronic phase, which is not observed under compression, could be realized.

Figure 2(d) shows the results when strain is applied along the b-axis. In the high-temperature region, the resistance decreases under compressive strain and increases under tensile strain, similar to the behavior observed under the a-axis strain. However, a significant change in resistance associated with the CO transition was not observed under tensile strain. Additionally, at low temperatures below approximately 120 K, the strain dependence of the resistance exhibits the opposite tendency: the resistance decreases under tensile strain along the b-axis. This result appears to be caused by the Poisson effect, which refers to the phenomenon

where compression (expansion) induces slight expansion (compression) in the perpendicular direction. As previously mentioned, this compound is sensitive to the a-axis strain. The compressive effect along the a-axis, induced by the Poisson effect during the application of the b-axis tensile strain, shifts T_{CO} to lower temperatures and results in lower resistance. Thus, the influence of the Poisson effect should be taken into consideration when discussing the experimental results under the b-axis strain, especially at low temperatures. These results indicate a large anisotropy in the effect of uniaxial strain direction. The fact that the CO insulating state is more easily controlled by the a-axis strain than by the b-axis strain is consistent with previous studies using clamp-type cell and substrate bending.[8,19)]

Next, we investigated the resistance as a function of uniaxial strain. The sample was first compressed uniaxially at a constant temperature and then expanded along the same direction. Our experimental method enables continuous strain application at low temperatures and in-situ resistance measurements. This is the first time such measurements have been performed on this compound, and the results allow us to investigate the details of the M–I transition. Figure 3(a) shows the a-axis strain dependence of the resistance of α-(BEDT-TTF)$_2$I$_3$. At high temperatures, the resistance varies linearly with strain. As the temperature decreases, the resistance becomes nonlinear with strain and changes drastically near T_{CO}. This behavior indicates a transition from a low-resistance metallic state to a high-resistance CO state. Thus, we successfully induced the CO state through uniaxial strain, demonstrating the effectiveness of the uniaxial strain in controlling the electronic state of organic conductors. Around T_{CO}, we note that the electrical resistance initially increases slightly with tensile strain, then remains nearly constant, and subsequently rises significantly. This behavior suggests the existence of a region where the resistance is less affected by strain.

Figure 3(b) shows the resistance of α-(BEDT-TTF)$_2$I$_3$ as a function of the b-axis strain at various temperatures. Compared to the results under the a-axis strain, the change in resistance is smaller. At temperatures near T_{CO}, a stepwise increase in resistance is observed. Since the resistance values are reproducible, this behavior is not caused by cracks in the sample. The resistance step appears under weaker tensile strain at lower temperatures. This structure is likely related to the structural phase transition accompanying the CO transition, as discussed later.[20)] The reason why the resistance does not increase significantly after the stepwise increase is probably due to the a-axis compressive strain resulting from the Poisson effect.

Next, we focus on the low-strain region. Figures 4(a) and 4(b) show the a- and the b-axes strain dependence of the sample resistance normalized by its value without strain, respectively. Here, the strain ϵ is estimated as $\epsilon = (1/K)\Delta R_g/R_g$ using the strain gauge resistance R_g, where ΔR_g is the change in resistance from its value without strain, and K is 2.1 for our gauge. The normalized sample resistance is linear with strain in the low-strain region, and its slope, $d(\Delta R/R)/d\epsilon$, is defined as the elastoresistance, which reflects the sensitivity of the electronic system to strain. Figure 4(c) shows the elastoresistance as a function of temperature for strain along the a-axis (red filled circles) and the b-axis (blue

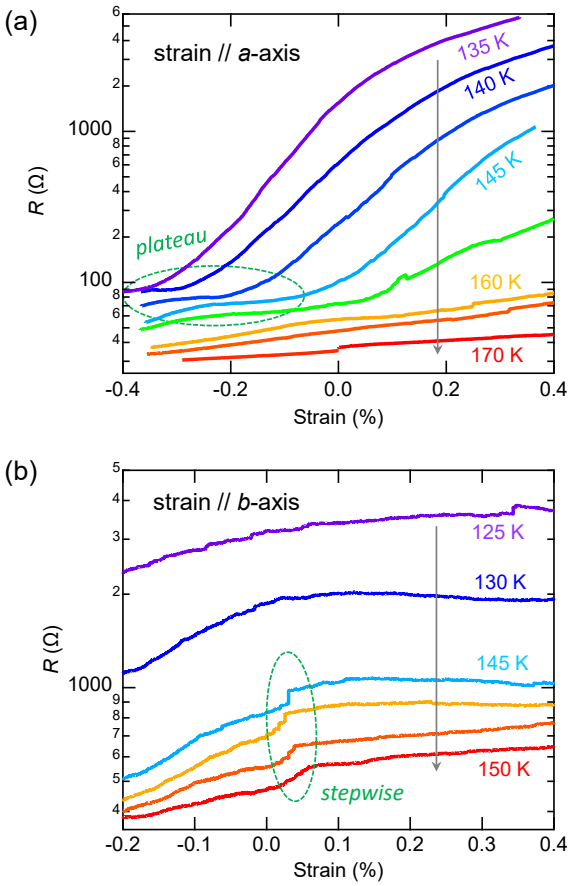

Fig. 3. (Color online) Resistance as a function of uniaxial strain along (a) the a-axis and (b) the b-axis. The green dotted lines in (a) and (b) indicate the regions where plateau-like structures and stepwise increases in resistance were observed, respectively.

open circles), respectively. For reference, the temperature dependence of resistance (black line) is also plotted on the right axis. As the temperature decreases, the elastoresistance decreases monotonically under the b-axis strain. On the other hand, under the a-axis strain, the elastoresistance initially increases with decreasing temperature but decreases slightly around 160 K before increasing divergently from 140 K, very close to T_{CO}. This result indicates the existence of a temperature region where the electronic system becomes insensitive to strain before the CO transition. The elastoresistance also exhibits anisotropy, although detailed discussion is difficult because the Poisson effect becomes non-negligible below T_{CO} under the b-axis strain.

Organic conductors generally have highly anisotropic crystal structures. In α-(BEDT-TTF)$_2$I$_3$, anisotropy exists in the orientation of BEDT-TTF molecules within the conduction plane, as shown in Fig. 2(a). The stacking direction of the molecules corresponds to the a-axis, while the inter-columnar direction corresponds to the b-axis. Electrical conduction is carried by π electrons that extend perpendicularly from the nearly flat BEDT-TTF molecules. Consequently, the electronic state is highly sensitive to molecular orientation, resulting in significant anisotropy in response to applied strain.

The crystal structure of α-(BEDT-TTF)$_2$I$_3$ before and after the CO transition was precisely elucidated by synchrotron X-ray diffraction measurements.[20)] These results revealed that

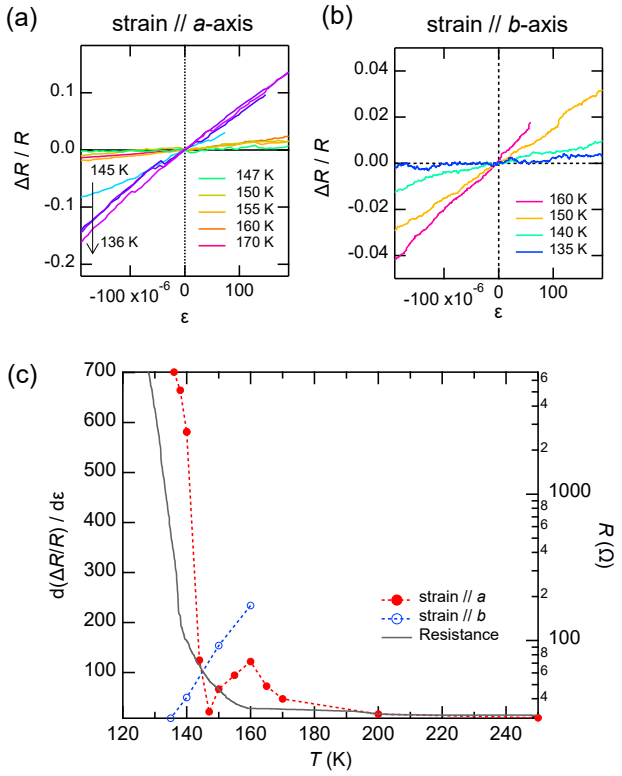

Fig. 4. (Color online) (a, b) Strain dependence of the normalized resistance along (a) the *a*-axis and (b) the *b*-axis, respectively. (c) elastoresistance as a function of temperature under the *a*-axis (red) and the *b*-axis (blue) strain. For reference, the temperature dependence of resistance (black) is plotted on the right axis.

the CO transition is accompanied by a structural phase transition, and the main structural change is not the translational shift of the BEDT-TTF molecules but a change in the dihedral angle θ, as defined in Fig. 2(b). The change in the angle θ affects the spatial overlap of the wave functions, leading to a drastic change in the transfer integrals during the CO transition, which ultimately results in a M–I transition.

Raman spectroscopy measurements show the presence of several low-energy phonons in this system, including the libration of BEDT-TTF molecules.[21,22] Here, the libration of molecules refers to the restricted rotational motion of the molecules around an equilibrium position. The libration of the BEDT-TTF molecules induces vibrations of the dihedral angle θ. As indicated by the X-ray diffraction measurements,[20] changes in the dihedral angle θ affect the transfer integral. Since specific heat measurements have shown that the M–I transition is first-order,[23] there is a region where the metallic and CO phases coexist. The double peak observed in X-ray diffraction measurements and the scanning near-field optical microscopy image[24] also suggest the coexistence of the two phases in the vicinity of T_{CO}. In this region, libration around the two equilibrium positions is likely to occur, leading to a broader spatial overlap of the wave function due to the increased angular range of rotational motion. As a result, the bandwidth is expected to be effectively broadened, reducing its sensitivity to tensile strain. Consequently, the resistance shows little variation with strain in the region where the two phases coexist, which may explain the plateau structure observed in Fig. 3(a). Similarly, the behavior observed in Fig. 4(c), where the elastoresistance becomes insensitive to the *a*-axis strain near T_{CO}, could be attributed to the same mechanism.

We speculate that by inducing a first-order phase transition from the metallic to the CO state through the application of uniaxial strain, we could observe these phenomena because the electronic state of this compound is sensitive to the libration of BEDT-TTF molecules, the importance of which has already been pointed out.[25,26] Further improvement in the sample setting, where a portion of the sample surface is exposed, would allows X-ray and Raman spectroscopy measurements, leading to a deeper understanding of the strain-induced phase transitions.

Acknowledgment This work was supported by JSPS KAKENHI Grants (No. 22K22444). MANA is supported by World Premier International Research Center Initiative (WPI), MEXT, Japan.

*KONOIKE.Takako@nims.go.jp

1) C. W. Hicks, M. E. Barber, S. D. Edkins, D. O. Brodsky, and A. P. Mackenzie, Rev. Sci. Instrum. **85**, 065003 (2014).
2) C. W. Hicks, D. O. Brodsky, E. A. Yelland, A. S. Gibbs, J. A. N. Bruin, M. E. Barber, S. D. Edkins, K. Nishimura, S. Yonezawa, Y. Maeno, and A. P. Mackenzie, Science **344**, 283 (2014).
3) I. Kostylev, S. Yonezawa, and Y. Maeno, J. Appl. Phys. **125**, 082535 (2019).
4) I. Kostylev, S. Yonezawa, Z. Wang, Y. Ando, and Y. Maeno, Nat. Commun. **11**, 4152 (2020).
5) J. M. Bartlett, A. Steppke, S. Hosoi, H. Noad, J. Park, C. Timm, T. Shibauchi, A. P. Mackenzie, and C. W. Hicks, Phys. Rev. X **11**, 021038 (2021).
6) M. Maesato, Y. Kaga, R. Kondo, and S. Kagoshima, Rev. Sci. Instrum. **71**, 176 (2000).
7) M. Suda, Y. Kawasugi, T. Minari, K. Tsukagoshi, R. Kato, and H. M. Yamamoto, Adv. Mater. **26**, 3490 (2014).
8) Y. Kawasugi, H. Suzuki, H. M. Yamamoto, R. Kato, and N. Tajima, Appl. Phys. Lett. **122**, 123102 (2023).
9) S. Katayama, A. Kobayashi, and Y. Suzumura, J. Phys. Soc. Jpn. **75**, 054705 (2006).
10) N. Tajima, S. Sugawara, M. Tamura, Y. Nishio, and K. Kajita, J. Phys. Soc. Jpn. **75**, 051010 (2006).
11) K. Bender, I. Hennig, D. Schweitzer, K. Dietz, H. Endres, and H. J. Keller, Mol. Cryst. Liq. Cryst. **108**, 359 (1984).
12) K. Bender, K. Dietz, H. Endres, H. W. Helberg, I. Henning, H. J. Keller, H. W. Schafer, and D. Schweitzer, Mol. Cryst. Liq. Cryst. **107**, 45 (1984).
13) H. Kino and H. Fukuyama, J. Phys. Soc. Jpn. **64**, 1877 (1995).
14) H. Seo, J. Phys. Soc. Jpn. **69**, 805 (2000).
15) Y. Takano, K. Hiraki, H. M. Yamamoto, T. Nakamura, and T. Takahashi, J. Phys. Chem. Solids **62**, 393 (2001).
16) T. Takahashi, Synth. Met. **133–134**, 261 (2003).
17) T. Ojiro, K. Kajita, Y. Nishio, H. Kobayashi, A. Kobayashi, R. Kato, and Y. Iye, Synth. Met. **56**, 2268 (1993).
18) N. Tajima, M. Tamura, Y. Nishio, K. Kajita, and Y. Iye, J. Phys. Soc. Jpn. **69**, 543 (2000).
19) N. Tajima, A. Ebina-Tajima, M. Tamura, Y. Nishio, and K. Kajita, J. Phys. Soc. Jpn. **71**, 1832 (2002).
20) T. Kakiuchi, Y. Wakabayashi, H. Sawa, T. Takahashi, and T. Nakamura, J. Phys. Soc. Jpn. **76**, 113702 (2007).
21) K. I. Pokhodnia, A. Graja, M. Weger, and D. Schweitzer, Z. Phys. B **90**, 127 (1993).
22) A. Graja, Synth. Met. **56**, 2477 (1993).
23) N. A. Fortune, K. Murata, M. Ishibashi, M. Tokumoto, N. Kinoshita, and H. Anzai, Solid State Commun. **79**, 265 (1991).
24) A. Pustogow, A. S. McLeod, Y. Saito, D. N. Basov, and M. Dressel, Sci. Adv. **4**, eaau9123 (2018).
25) S. Iwai, K. Yamamoto, A. Kashiwazaki, F. Hiramatsu, H. Nakaya, Y. Kawakami, K. Yakushi, H. Okamoto, H. Mori, and Y. Nishio, Phys. Rev. Lett. **98**, 097402 (2007).
26) S. Iwai, K. Yamamoto, F. Hiramatsu, H. Nakaya, Y. Kawakami, and K. Yakushi, Phys. Rev. B **77**, 125131 (2008).